Journal of Molecular Catalysis A: Chemical 301 (2009) 106–113

Contents lists available at ScienceDirect

Journal of Molecular Catalysis A: Chemical

journal homepage: www.elsevier.com/locate/molcata

Synthesis of ethylbenzene by alkylation of benzene with diethyl carbonate over parent MCM-22 and hydrothermally treated MCM-22

Yongxin Li*, Bing Xue, Xueyi He

College of Chemistry and Chemical Engineering, Jiangsu Polytechnic University, Changzhou, Jiangsu 213164, China

ARTICLE INFO

Article history:
Received 5 August 2008
Received in revised form
14 November 2008
Accepted 17 November 2008
Available online 25 November 2008

Keywords:
Diethyl carbonate
Alkylation
Benzene
MCM-22

ABSTRACT

Acidity adjustment of MCM-22 was carried out by hydrothermal treatment of parent MCM-22 with flowing pure steam at high temperature. XRD, SEM and N_2 adsorption/desorption results indicated that the crystallinity and pore properties of MCM-22 were affected slightly by hydrothermal treatment at different temperatures. NH_3-TPD and FT-IR with pyridine adsorption showed only a slight decrease in Brønsted acid sites, compared with parent MCM-22, with hydrothermal treatment temperature in the range 773–873 K. The strength of Brønsted acid sites was reduced severely at hydrothermal treatment temperatures of 973 and 1073 K. The Lewis acid sites were only slightly affected by hydrothermal treatment. A substantial improvement in ethylbenzene selectivity along with a slight decrease in benzene conversion was achieved in catalytic synthesis of ethylbenzene by alkylation of benzene with diethyl carbonate over MCM-22 hydrothermally treated at 873 K. A sharp decrease in benzene conversion was detected over MCM-22 hydrothermally treated at 973 K. The results indicate that alkylation of benzene with diethyl carbonate occurred mainly on Brønsted acid sites, and the effect of Lewis acid sites on the alkylation process is negligible. Reduction of Brønsted acid sites of the catalyst can suppress side reactions and improve selectivity for ethylbenzene. It was found that a particular acid strength of catalyst was required to maintain high benzene conversion and ethylbenzene selectivity.

1. Introduction

MCM-22 possesses two independent pore systems. The first consists of two dimensional channels with 10 membered ring openings, while the other comprises large super cages of 12 membered rings with dimensions 7.1 Å × 7.1 Å × 18.2 Å [1,2]. The major advantages of MCM-22 are its high thermal stability, high acid-catalysis activity and good molecular shape selectivity [3–5]. Recently, MCM-22 has been applied to commercial processes for ethylbenzene and cumene production by alkylation of benzene with ethylene and propylene [6,7].

Alkylation of benzene is an important reaction in the petrochemical industry [8,9]. As the most important alkylbenzene, ethylbenzene (EB) is predominantly synthesized by alkylation of benzene with ethylene using ZSM-5 and MCM-22 as acid catalysts. Conventionally, ethylene as feedstock for synthesis of EB is produced from naphtha steam cracking. With continuous development of the world's economy, oil demand is increasing rapidly, causing a rising price of ethylene. Known petroleum reserves are limited resources, estimated to be depleted in less than 50 years at the present rate of consumption [10]. In recent years, there has been a strong increase in production of EB in the world, and this trend will be maintained in the future. Consequently investigations have been carried out on synthesis of ethylbenzene using other alkylating agents as a substitute for ethylene. Use of ethanol as a substitute for ethylene in synthesis of EB by alkylation of benzene with ethanol has been investigated [8]. A high molar ratio of benzene to ethanol is required to ensure good catalyst lifetime in the alkylation process. However, a high molar ratio of benzene to ethanol results in low conversion of benzene, which may cause a large quantity of unconverted benzene to be circulated in the industrial process, and results in increased energy consumption [11]. Diethyl carbonate (DEC) is a versatile compound that represents an attractive ecofriendly alternative to ethyl halides and phosgene for ethylation and carbonylation processes, respectively [12,13]. Our experimental results indicated that by using DEC as ethylation agent, high conversion of benzene was obtained in alkylation of benzene with DEC over ZSM-5 catalyst, and a good catalyst lifetime was maintained. To the best of our knowledge there are no reports on the use of DEC as ethylating agent to synthesize EB.

Both the activity and selectivity of zeolite for alkylation reactions such as alkylation of benzene with ethylene are directly related to catalyst acidity; and hydrothermal treatment is usually employed to adjust zeolite acidity by de-alumination [14–18]. In the present study, the catalytic performance of parent MCM-22 and MCM-22

* Corresponding author. Tel.: +86 519 86330135; fax: +86 519 86330135.
E-mail address: liyx@em.jpu.edu.cn (Y. Li).

1381-1169/$ – see front matter © 2008 Published by Elsevier B.V.
doi:10.1016/j.molcata.2008.11.018

de-aluminated by hydrothermal treatment, in synthesis of EB by alkylation of benzene with DEC, was investigated. In addition, a comparison of ZSM-5 and MCM-22 for alkylation of benzene with DEC was carried out.

2. Experimental

2.1. Catalyst preparation

MCM-22 zeolites with Si/Al ratio = 50 were synthesized by hydrothermal crystallization according to the reported procedure [19]. The NH_4 form of the as-synthesized zeolites was obtained by ion-exchange with aqueous NH_4NO_3 solution. The acidic form of MCM-22 zeolite was prepared by calcination at 823 K for 3 h. Hydrothermal treatment was carried out on MCM-22 zeolite in a fixed bed reactor at various temperatures with pure steam (WHSV 0.3 h^{-1}) for 4 h. The samples were treated with pure steam at 773, 873, 973 and 1073 K and are denoted HTM-7, HTM-8, HTM-9 and HTM-10, respectively.

2.2. Catalyst characterization

X-ray diffraction (XRD) measurements were conducted using a Rigaku D/max2500PC diffractometer with Cu Kα (λ = 1.54 Å) radiation. The diffractograms were recorded in the 2θ range 5–40° in steps of 0.02° with a count time of 15 s. SEM images of the MCM-22 and hydrothermally treated MCM-22 were obtained for structural identification using a JSM-6360LA scanning electron microscope. N_2 adsorption/desorption analyses were obtained at 77 K using a physical adsorption instrument (Micromeritics ASAP 2010, USA). Before measurement, the samples were degassed at 523 K under vacuum until a final pressure of 1×10^{-3} kPa was reached. The specific surface area was calculated according to the BET isothermal equation.

Chemical composition of the samples was determined by Inductively Coupled Plasma Optical Emission Spectrometry (ICP-OES) using a PerkinElmer Optima 4300DV instrument. Samples were pre-dissolved and digested in an HF 10%/HCl–HNO_3 (1:3) mixture.

FT-IR spectra of the samples were recorded using a Bruker FT-IR spectrometer (TENSOR 27) with the KBr pellet technique. Spectra were recorded in the range 4000–400 cm^{-1}. IR spectroscopy with pyridine adsorption was carried out using the same instrument together with a high temperature vacuum chamber. The scanning range was 1700–1400 cm^{-1} and the resolution was 4 cm^{-1}. The sample powder was pressed into a self-supporting wafer. Prior to each experiment, the catalysts were evacuated (1 Pa) at 653 K for 3 h. They were then cooled at 303 K for 2 h, then the material was exposed to 30 Torr of pyridine for 5 min, and finally evacuated for 1 h at 303 K. After adsorption of pyridine the samples were heated to 473 and 653 K at 10 K min^{-1} and the spectra recorded.

Sample acidity was measured by NH_3 temperature-programmed desorption (NH_3-TPD) using a Quantachrome CHEMBET-3000 instrument. A 200 mg sample was pre-treated at 823 K for 1 h in dry helium (flowing at 50 ml min^{-1}), cooled to 393 K, then exposed to 10% (v/v) NH_3/He mixture for 0.5 h. After purging the catalyst with He for 0.5 h, the TPD plot was obtained at a heating rate of 10 K min^{-1} from 393 to 823 K. The thermal conductivity detector (TCD) signal and temperature corresponding to NH_3 desorption were recorded simultaneously. The amount and temperature of the desorbed NH_3 corresponded qualitatively to the amount and strength of the acid sites.

2.3. Ethylation of benzene with DEC

Vapor phase alkylation of benzene with DEC was carried out in a fixed bed continuous down-flow reactor. Five milliliters of the catalyst (in the form of 20–30 mesh pellets) was loaded in the middle of the reactor fitted with a thermocouple for temperature measurement. The reactor was heated to the requisite temperature in a tubular furnace controlled by a digital temperature controller/indicator. The reaction mixture of benzene and DEC was introduced at the top of the reactor by means of an infusion pump. The products were collected in a water-cooled condenser attached to the end of the reactor and analyzed by gas chromatography (SP-6890, China) using a polyglycol-packed column (d = 3 mm) and flame ionization detector (FID). The catalysts were tested for 10 h on stream, and conversions were compared after the steady state was attained. The percentage conversion was calculated based on benzene.

3. Results and discussion

3.1. Characterization

3.1.1. Physicochemical properties of samples

XRD patterns of the samples are shown in Fig. 1. The number and position of peaks correspond to the specific peaks of MCM-22 zeolite [20] and do not change with the temperature of hydrothermal treatment. The high intensity of peaks in the XRD patterns indicated that the zeolite samples were highly crystalline. The intensity of the peaks increased slightly as hydrothermal treatment temperature increased from 773 to 873 K: that effect has been demonstrated to be due to the removal of framework Al from MCM-22 [21]. A slight decrease in peak intensity was, however, observed for HTM-9 and HTM-10, which suggests that slight loss of crystallinity occurred at higher hydrothermal treatment temperatures.

Fig. 2 shows SEM images of MCM-22 and MCM-22 hydrothermally treated at 1073 K. In Fig. 2 aggregates of platelets with irregular shape are prominent. The platelets do not have well defined morphologies and most of the platelets appear to be more than 1 μm in size, which was also reported by Unverrichet et al. [22] and Dahlhoff et al. [23]. No significant changes associated with hydrothermal treatment were observed in the SEM images.

Mid-infrared FT-IR spectra of MCM-22 and hydrothermal treated samples are shown in Fig. 3. The positions of the vibrational bands for all of the samples are in agreement with IR spectra reported elsewhere [24]. The weak, broad envelope between 2500 and 3700 cm^{-1} is assigned to OH stretching of defective Si-OH and Al-OH (belonging to extra-framework Al) groupings [25]. A decrease in intensity of these vibrations was observed with increase in the tem-

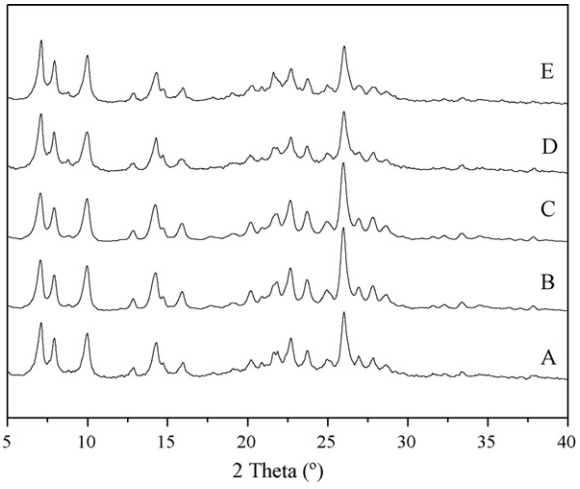

Fig. 1. X-ray diffraction of parent MCM-22 and hydrothermally treated MCM-22 catalysts. (A) Parent MCM-22; (B) HTM-7; (C) HTM-8; (D) HTM-9; (E) HTM-10.

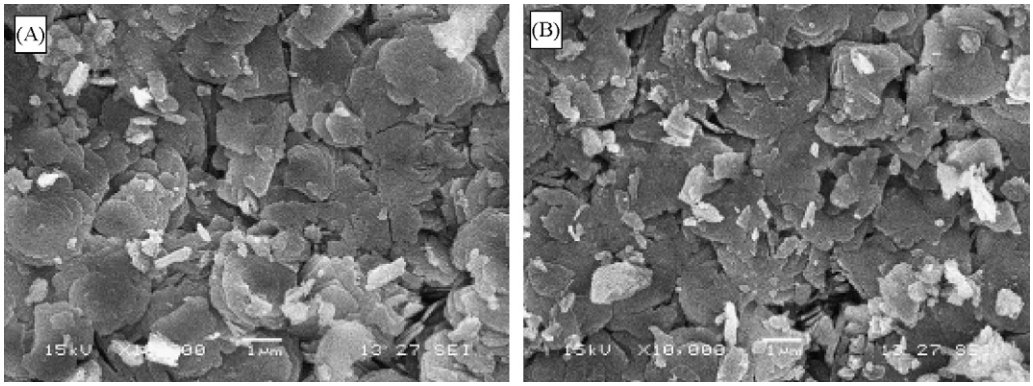

Fig. 2. SEM images of parent MCM-22 and hydrothermally treated MCM-22 catalysts. (A) Parent MCM-22; (B) HTM-10.

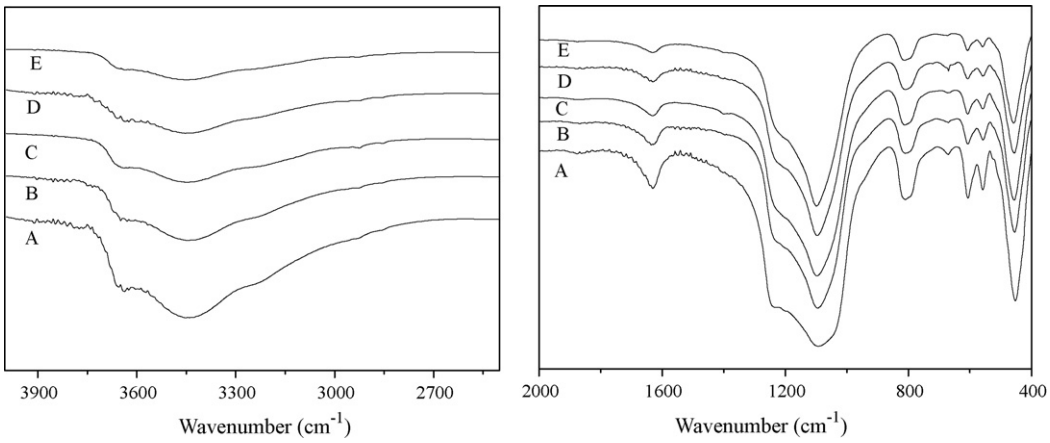

Fig. 3. FT-IR spectra of parent MCM-22 and hydrothermally treated MCM-22 catalysts. (A) Parent MCM-22; (B) HTM-7; (C) HTM-8; (D) HTM-9; (E) HTM-10.

perature of hydrothermal treatment, suggesting de-alumination resulting from the hydrothermal treatment. The band corresponding to the asymmetric stretch of internal tetrahedral (1082 cm^{-1}) shifted to higher wavenumber (1092 cm^{-1}) with increase in the temperature of hydrothermal treatment, indicating decrease in aluminum content [26].

N_2 adsorption/desorption analysis is a useful tool for examining textural characteristics of porous materials. The isotherms for parent MCM-22 and MCM-22 hydrothermally treated at 1073 K are displayed in Fig. 4. The isotherms of the two samples are similar with a hysteresis loop at relatively high pressure (p/p_0), indicating that the crystal sizes are small and present a relatively high external surface area with little mesoporosity [27]. It can be deduced that the hydrothermal treatment at different temperatures has little influence on the basic porous structure of parent MCM-22 zeolite, which is consistent with the XRD results. The textural parameters of the corresponding samples are summarized in Table 1. The parent MCM-22 has high BET surface area (357.9 $m^2\ g^{-1}$), which can be attributed to large supercages in MCM-22 zeolites [28]. The BET surface area and micropore area decrease markedly with higher treatment temperatures, and the average pore diameter shows the reverse trend. It is apparent that the hydrothermal treatment has a pronounced effect on the pore properties of MCM-22, especially for HTM-10. Hydrolysis of Si–O–Al bonds and removal of framework Al occurred during the hydrothermal treatment process, resulting in partially destroyed and blocked micropores [18].

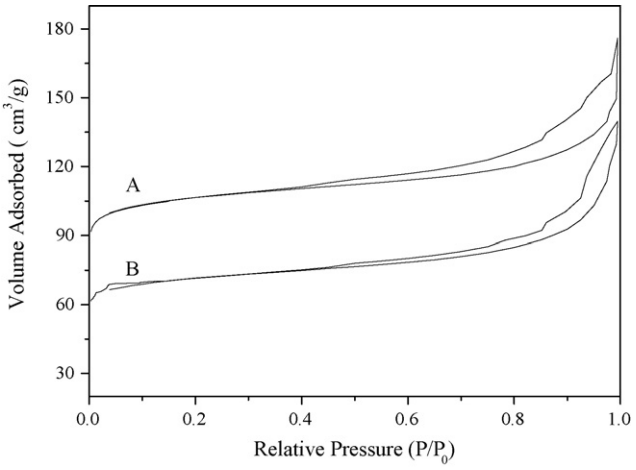

Fig. 4. N_2 adsorption/desorption isotherms of parent MCM-22 and hydrothermally treated MCM-22 catalysts. (A) Parent MCM-22; (B) HTM-10.

3.1.2. Acid properties of samples

Fig. 5 shows the NH_3-TPD spectra of parent MCM-22 and hydrothermally treated MCM-22. The spectrum of the parent MCM-22 exhibits typical double peak characteristics of zeolites with MFI structures [20]. The strong peak at 500 K is attributed to desorption of adsorbed ammonia from weakly acidic sites, and the weak peak at 700 K is assigned to desorption of adsorbed ammonia from strongly acidic sites. The number of weakly acidic sites was obviously greater than the number of strongly acidic sites in MCM-22. The acid strength of both the strongly acidic and weakly acidic sites decrease markedly with increase in treatment temperature. The strongly acidic sites almost disappear when the treatment temper-

Table 1
Textural parameters of parent MCM-22 and hydrothermally treated MCM-22 catalysts.

Sample	A_{BET}/m^2 g^{-1}	A_M/m^2 g^{-1}	A_E/m^2 g^{-1}	V_T/cm^3 g^{-1}	V_M/cm^3 g^{-1}	D_A/nm
MCM-22	357.9	289.6	68.3	0.216	0.135	2.41
HTM-7	285.8	222.5	63.3	0.186	0.103	2.60
HTM-8	276.1	214.8	61.3	0.176	0.098	2.62
HTM-9	262.6	204.1	58.5	0.176	0.095	2.68
HTM-10	240.9	185.9	55.0	0.175	0.087	2.92

A_{BET}, BET surface area; A_M, micropore area; A_E, external surface area; V_T, total pore volume; V_M, micropore volume; D_A, average pore diameter.

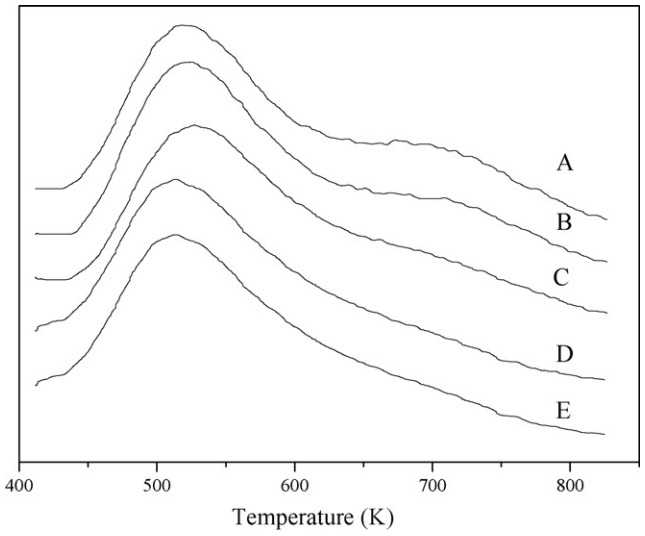

Fig. 5. NH_3-TPD spectra of parent MCM-22 and hydrothermally treated MCM-22 catalysts. (A) Parent MCM-22; (B) HTM-7; (C) HTM-8; (D) HTM-9; (E) HTM-10.

ature is higher than 973 K, while the weakly acidic sites are still prominent even on HTM-10 samples.

The acid properties of MCM-22 and the hydrothermally treated MCM-22 were examined by FT-IR spectroscopy using the pyridine-adsorption technique at different temperatures, as shown in Fig. 6. The band at 1450 cm^{-1} is due to pyridine adsorbed on Lewis acid sites, while pyridine adsorbed on Brønsted acid sites gives the band at 1540 cm^{-1}. The combination of Lewis and Brønsted acid sites is manifested in a band at 1490 cm^{-1}. Fig. 6 shows that the intensity of the band at 1540 cm^{-1} decreases slightly with increase in treatment temperature from 773 to 873 K. A sharp decrease was observed in the intensity of the band at 1540 cm^{-1} when the temperature was above 1073 K, indicating that many Brønsted acid sites were eliminated by hydrothermal treatment at temperatures above 1073 K. Hydrothermal treatment at different temperatures did not seem to have a significant effect on the intensity of Lewis acid sites. The results from the FT-IR spectra of adsorbed pyridine recorded at different evacuation temperatures are given in Table 2. The total number of Brønsted acid sites was reduced slightly when hydrothermal treatment was carried out below 873 K; treatment at higher temperatures markedly reduced the total number of Brønsted acid sites. A decrease in the B/L ratio is apparent in all of the FT-IR spectra of adsorbed pyridine, especially for HTM-9 and HTM-10, indicating that Brønsted acid sites were lost to a greater extent than Lewis acid sites.

The Si/Al ratios for parent MCM-22 and hydrothermally treated MCM-22 are also listed in Table 2. The Si/Al ratio clearly increases after hydrothermal treatment, suggesting that most of the Al atoms in the de-aluminated samples were removed. In addition, the HTM-10 sample has less than 60% of the Al content of the parent MCM-22.

It is known that the acidity of zeolite depends on the framework Si/Al ratio either during synthesis or post-treatment de-alumination [29]. Hydrothermal treatment is the most common de-alumination technique used to prepare industrial catalysts [30]. The number of framework Al atoms, which contribute to the strength of Brønsted acid sites, can be reduced severely by hydrothermal treatment at high temperature [31]. The removal of Al atoms from the zeolite framework can arise from hydrolysis of the Si–O–Al bonds. As shown in Table 2, for HTM-10 about 75% of initial Brønsted acid sites were removed by de-alumination, while only about 40% of the initial Al atoms were extracted, indicating that some Al species may have migrated from the framework to form extra-framework Al species that can dissolve easily in water [32]. Guo et al. reported that the signal intensity of Al detected by NMR decreased after hydrothermal treatment, indicating that removal of Al from lattice occurred and NMR-invisible extra-lattice Al species was produced [18]. With decrease in framework Al content, the acidic strength of MCM-22 sharply decreases as shown in the NH_3-TPD profile, which has been reported in the literature [18]. The significant decrease in Brønsted acidic sites indicated that the framework Al contributed to the strength of Brønsted acidic

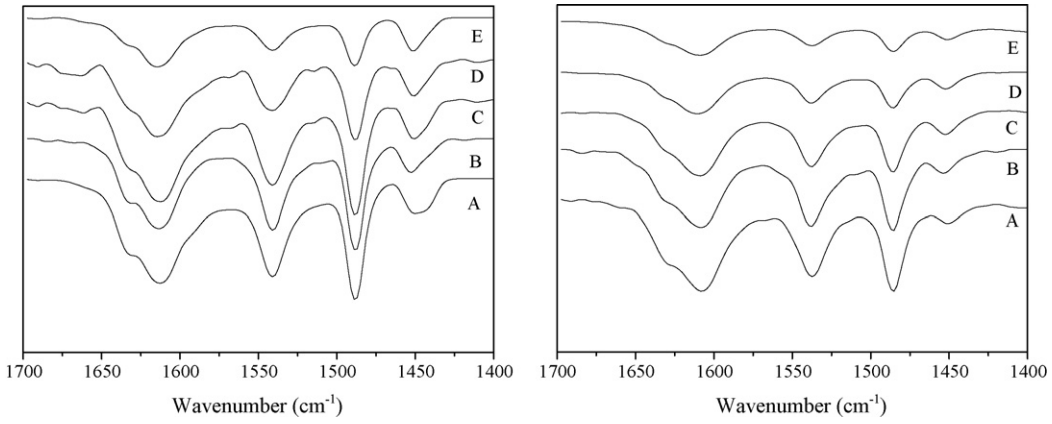

Fig. 6. FT-IR spectra of parent MCM-22 and hydrothermally treated MCM-22 catalysts after adsorption of pyridine and evacuation at 473 K (left) and 673 K (right). (A) parent MCM-22; (B) HTM-7; (C) HTM-8; (D) HTM-9; (E) HTM-10.

Table 2
Results of FT-IR spectra of parent MCM-22 and hydrothermally treated MCM-22 catalysts after adsorbing pyridine and evacuating.[a].

Sample		FT-IR spectroscopy of adsorbed pyridine					
		473 K		673 K		B/L	
	Si/Al[b]	B	L	B	L	473 K	673 K
MCM-22	49	1.17	0.46	0.66	0.09	2.54	7.33
HTM-7	53	0.98	0.38	0.50	0.09	2.58	5.56
HTM-8	57	0.96	0.37	0.43	0.08	2.59	5.37
HTM-9	66	0.76	0.35	0.21	0.08	2.17	2.63
HTM-10	79	0.37	0.31	0.16	0.08	1.19	2.00

[a] The number of acid sites is the relative value of Brønsted acid and Lewis acid sites, estimated from the corresponding calibrated peak areas.
[b] Measured by ICP-OES.

sites, while the strength of Lewis acidic sites is associated with the extra-framework aluminum species, as reported by Beyer [30]. But in the corresponding FT-IR spectra, the strength of Lewis acid site does not increase obviously. On the contrary, it decreases at higher hydrothermal treatment temperatures. This may be due to the condensation of extra-framework aluminum hydroxyls to polymeric aluminum species [33,34]. In addition, it has been reported that only a part of the extra-framework aluminum acts as Lewis acid sites [35].

3.2. Catalytic activity evaluation

Fig. 7 shows benzene conversion in alkylation of benzene with DEC over parent MCM-22 and hydrothermally treated MCM-22. The conversion of benzene decreases slightly over HTM-7 and HTM-8 compared with the parent MCM-22, while a sharp decline in benzene conversion was observed over HTM-9. Catalytic synthesis of EB by benzene alkylation has been mostly regarded as a typical acid-catalyzed process requiring the presence of Brønsted acid sites on the catalyst surface [36]. The strong surface acidity of MCM-22 favors the alkylation reaction. According to the acid properties and strength characterization (shown in Fig. 5 and Table 2), the parent MCM-22 exhibits the strongest acidity among the investigated catalysts and correspondingly the highest benzene conversion. Though the total strength of acid sites decreases slightly with increase in the temperature of hydrothermal treatment, most of the Brønsted acid sites were retained on HTM-7 and HTM-8. Thus only a slight decrease of benzene conversion over HTM-7 and HTM-8 was detected. A rapid decline in Brønsted acid sites results in significant decrease in benzene conversion when the hydrothermal treatment temperature reaches 973 K. As shown in Fig. 7 the samples treated at 973 and 1073 K exhibit a high initial activity, but then a clear deactivation for HTM-9 and HTM-10 is observed. This effect may ascribe to the intense side reactions of oligomerization and coking. As shown in Table 2, a pronounced decrease in B/L ratio was obtained with increase in temperature of hydrothermal treatment, indicating that the proportion of Lewis acidic sites increases significantly. With decrease in Brønsted acid sites the alkylation of benzene to form EB was restricted, while the side reactions of oligomerization and coking were improved with increase in the proportion of Lewis acidic sites over deeply dealuminated samples. The increase in proportion of Lewis acid sites is supposed to be responsible for the fast deactivation over deeply samples [37]. Furthermore, the BET surface area and micropore surface area of the catalyst decreases largely, especially for HTM-10, which can also significantly affect the catalytic behavior in alkylation of benzene with DEC [30]. Moreover, the strength of Lewis acid sites was hardly affected by the temperature of hydrothermal treatment, confirming that the alkylation of benzene with DEC occurred mainly on Brønsted acid sites.

The EB selectivity and product distribution in the alkylation of benzene with DEC over parent MCM-22 and hydrothermally treated MCM-22 are presented in Fig. 8 and Table 3. The products identified by GC-MS were found to be EB, toluene, *para*-diethyl benzene (*p*-DEB), *ortho*-diethyl benzene (*o*-DEB), *meta*-diethyl benzene (*m*-DEB), triethyl benzene (TEB) and others (polyalkyl benzene). Benzene alkylation (including mono-alkylation and multi-alkylation), EB disproportionation and cracking, as well as DEB isomerization reactions co-existed during the alkylation process of benzene with DEC over parent MCM-22 and hydrothermally treated MCM-22. As shown in Fig. 8, a great improvement in EB selectivity was observed over HTM-8 compared with the parent

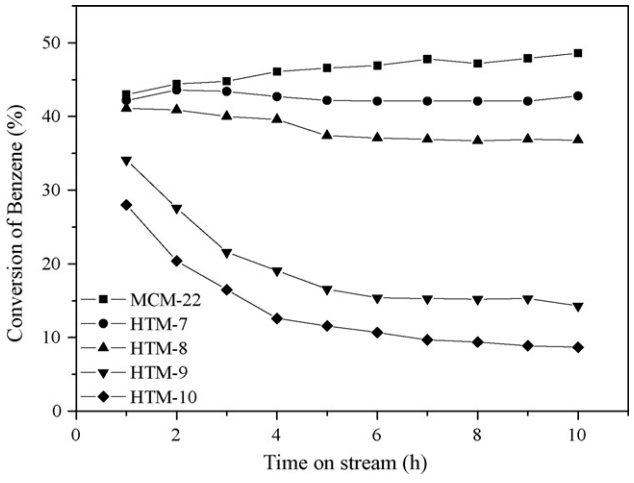

Fig. 7. Conversion of benzene on various catalysts. Conditions: temperature = 653 K; WHSV = 1.5 h^{-1}; feed ratio (benzene:DEC) = 4:1.

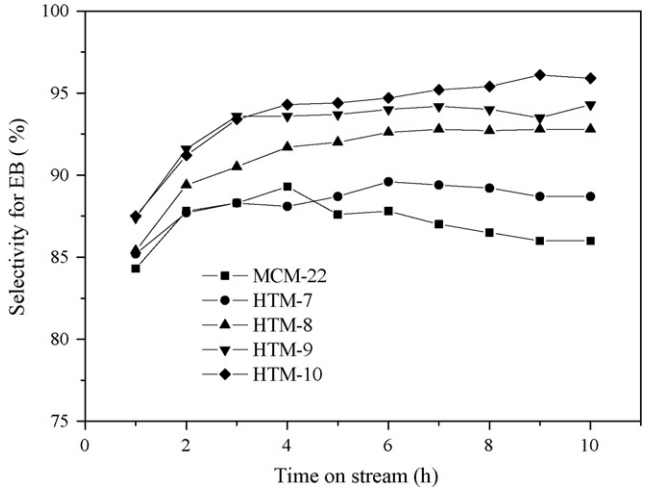

Fig. 8. Selectivity for EB on various catalysts. Conditions: temperature = 653 K; WHSV = 1.5 h^{-1}; feed ratio (benzene:DEC) = 4:1.

Table 3
Product distribution on various catalysts.[a].

Sample	Sel./%						
	EB	Toluene	*p*-DEB	*o*-DEB	*m*-DEB	TEB	Others
MCM-22	86.5	3.7	5.2	2.0	1.5	0.3	0.8
HTM-7	89.2	2.3	4.4	1.7	1.3	0.3	0.8
HTM-8	92.8	1.4	3.1	1.2	0.8	0.0	0.7
HTM-9	94.6	0.9	1.7	1.1	0.7	0.0	1.0
HTM-10	95.5	0.7	1.7	0.8	0.4	0.0	0.9

[a] Conditions: temperature = 653 K; WHSV = 1.5 h^{-1}; feed ratio (benzene:DEC) = 4:1.

MCM-22. With further increase in the temperature of hydrothermal treatment, the EB selectivity increases slightly. Though Brønsted acid sites were required for alkylation of benzene with DEC, excessively strong surface acidity of the catalysts is not favorable for EB selectivity [38]. From the acidity analysis above, the acid strength is reduced with increase in the temperature of hydrothermal treatment. With reduction in benzene multi-alkylation and ethylbenzene cracking reactions, high EB selectivity was obtained over hydrothermally treated MCM-22 catalysts, suggesting that these side reactions require much stronger acidity than does benzene mono-alkylation. It appears that some side reactions, such as benzene multi-alkylation and ethylbenzene cracking, were suppressed because of the reduced acidity strength. Although the highest EB selectivity was achieved over HTM-10, the activity for alkylation of benzene with DEC was poor. Thus only a certain acidity strength of catalyst was required in the synthesis of EB by alkylation of benzene with DEC.

As shown in Table 3, EB was obtained as the most predominant product over all of the catalysts, corresponding to free diffusion without steric hindrance through the pores of MCM-22. Among the DEB isomers, *p*-DEB shows the highest selectivity over all the investigated catalysts. The low selectivity for *o*-DEB might be due to steric hindrance to diffusion. The selectivity for *m*-DEB is low because the *meta*-position is not activated for electrophilic reaction. Consequently, electrophilic reaction occurs predominantly at the *para*-position as it is free from steric hindrance [39]. With increase in hydrothermal treatment temperature the selectivity for DEB isomers decreases substantially, corresponding to suppression of both EB multi-alkylation and *p*-DEB isomerization reactions. The selectivity for toluene decreases sharply with hydrothermal treatment temperature from 773 to 1073 K, indicating restriction of EB cracking reaction.

As mentioned above, a relationship between catalytic activity and acidic strength was revealed, which suggested that the weak acidity of de-aluminated MCM-22 is not favorable for the conversion of benzene, but favors highly selective synthesis of EB. To catalyze alkylation of benzene with DEC, strong acidity was required to activate the molecules of benzene and DEC. Consequently, conversion of benzene increases with increase in the acidity of the catalyst, and the strong acidity of parent MCM-22 results in high conversion of benzene. However, according to the product distribution shown in Table 3, the selectivity for EB significantly decreases with increase in the acidity of the catalyst, while the selectivity for toluene and DEB increase significantly. It has been reported that the acidic sites that catalyze EB multi-alkylation, EB cracking and DEB isomerization reactions are stronger than those that catalyze benzene mono-alkylation reaction. Those side reactions can be effectively suppressed with decrease in acidity. It follows that the conversion of benzene decreases significantly with decrease in acidic strength, while the selectivity for EB changes in the reversed order. According to this mechanism, a particular acidic strength was required to maintain good benzene conversion and EB selectivity. Accordingly, HTM-8 is a good candidate for the alkylation of benzene with DEC, exhibiting great improvement in EB selectivity along with a slight decrease in benzene conversion compared with parent MCM-22.

The product distribution and the selectivity obtained over MCM-22 and hydrothermally treated MCM-22 at similar benzene conversion level by adjusting contact time (WHSV), are shown in Table 4. The selectivity for EB increases with the degree of de-alumination, while the selectivity for other products, such as toluene and DEB, decreases with increase in the temperature of hydrothermal treatment. As discussed previously, the acidic sites required for catalyzing multi-alkylation, cracking of EB and isomerization of DEB, are stronger than those for catalyzing mono-alkylation of benzene. De-alumination treatment effectively removes the acidic sides on zeolites (Table 2). The removal of acidic sites may suppress the subsequent multi-alkylation and cracking of EB to give rise to the improved EB selectivity of hydrothermally treated MCM-22. Compared with the results shown in Fig. 7 and Table 3, for parent MCM-22 and HTM-7 conversion of benzene clearly decreases with decrease in contact time, while the selectivity for EB increases slightly. With decrease in contact time, the opportunity for activated benzene to be attacked by ethyl cation was of course reduced, leading to the decrease in conversion of benzene. EB can be selectively obtained by alkylation of benzene with DEC and the subsequent reactions of EB can be improved by strong acidic sites on the catalysts. The selectivity for EB was mainly affected by the side reactions including multi-alkylation, disproportionation and cracking of EB, as well as DEB isomerization reactions, which were influenced by the acidity of the catalysts. The effect of contact time on side reactions was weak, as shown in Fig. 7 and Table 3. It can be concluded that the influence of contact time on EB selectivity can be neglected compared with the change in acidic strength.

3.3. Alkylation of benzene with DEC over ZSM-5

Alkylation of benzene with DEC was carried out over ZSM-5 (Si/Al = 50), and the results are compared in Table 5 with those for alkylation over MCM-22. A substantial difference was found for the conversion of benzene, namely 35.6% over ZSM-5 and 43.1% over MCM-22. A stronger acidity can be detected on ZSM-5 compared with MCM-22 with similar Si/Al ratios. For this reason, higher benzene conversion is expected over ZSM-5, contrary to the experimental observations. Conversion of DEC detected by GC is over 99% in all the case, which is in similar to the conversion of ethylene in the alkylation of benzene with ethylene. As was reported that an approximate 100% ethylene conversion was achieved in the alkylation of benzene with ethylene [40]. The activated ethylene can easily reacted with another ethylene to form oligomers, a substance considered to be a precursor of coke, over acidic catalysts [36]. It was reported that dialkyl carbonates are easily decomposed over acid or basic materials, because the surface acidity or basicity plays an important role in their decomposition [41,42]. Dialkyl ether, as the predominant decomposition product of dialkyl carbonate, was much more difficult to give out alkyl cation compared with dialkyl carbonate. In addition, the decomposition of dialkyl

Table 4
Catalytic activity of benzene alkylation with DEC over various catalysts.[a].

Sample	WHSV/h^{-1}	Con./%	Sel./%						
		Benzene	EB	Toluene	*p*-DEB	*o*-DEB	*m*-DEB	TEB	Others
MCM-22	6.0	37.5	88.2	2.9	4.7	1.6	1.1	0.2	1.3
HTM-7	5.0	37.8	89.3	2.1	4.2	1.7	1.0	0.3	1.4
HTM-8	1.5	36.7	92.8	1.4	3.1	1.2	0.8	0.0	0.7

[a] Conditions: temperature = 653 K; feed ratio (benzene:DEC) = 4:1.

Table 5
Comparison of benzene alkylation with DEC over ZSM-5 and MCM-22.[a].

Samples	Con.%	Sel./%						
	Benzene	EB	Toluene	*p*-DEB	*o*-DEB	*m*-DEB	TEB	Others
ZSM-5	35.6	78.8	11.1	5.3	0.9	0.9	0.8	2.2
MCM-22	43.1	86.5	3.7	5.2	2.0	1.5	0.3	0.8

[a] Conditions: temperature = 653 K; WHSV = 1.5 h^{-1}; feed ratio (benzene:DEC) = 4:1.

carbonate increases greatly with increase in acidity of catalysts. Decomposition of DEC as a competitive reaction co-exists during the alkylation process of benzene with DEC. With the strong acidity of ZSM-5 decomposition of DEC may be substantially enhanced, resulting in lack of ethyl cation, and the reduced catalytic activity that was found. The selectivity for EB was lower over ZSM-5 (78.8%) than over MCM-22 (86.5%). As mentioned above, stronger acidity was favorable for side reactions such as multi-alkylation, disproportionation and cracking of EB, as well as DEB isomerization, compared with mono-alkylation of benzene with DEC. The strong acidity of ZSM-5, compared with MCM-22, facilitates multi-alkylation and cracking of EB, which results in the low selectivity for EB.

3.4. A possible mechanism

On the basis of the above discussion, a proposed mechanism for alkylation of benzene with DEC over MCM-22 and hydrothermally treated MCM-22 is illustrated in Scheme 1. First, DEC is chemisorbed on the Brønsted acid sites of the catalyst to yield the carbocation, then ethyl cations are produced with the rupture of the C–O bond. The second ethyl cation is obtained in a similar manner. Then an electrophilic reaction between ethyl cation and benzene occurs and the respective products are obtained with different selectivities. The residual carbonic acid may be decomposed to form CO_2 and water.

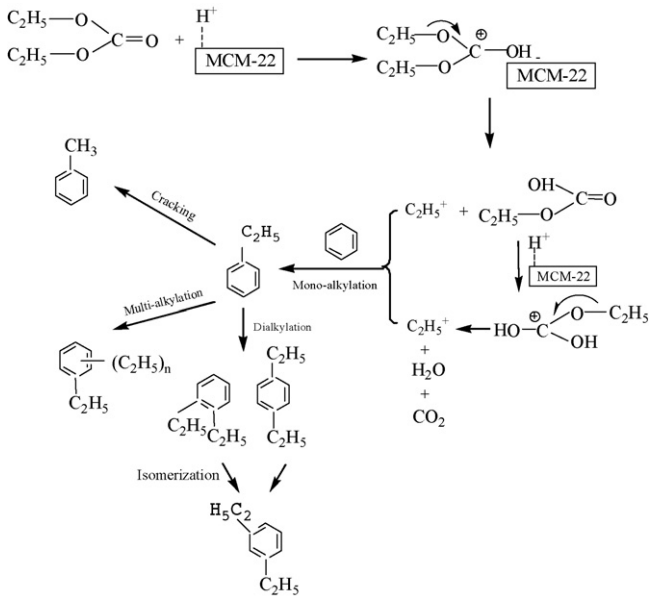

Scheme 1. A possible mechanism.

4. Conclusions

For MCM-22 zeolite, only a slight decrease in Brønsted acid sites is observed with variation of the hydrothermal treatment temperature from 773 to 873 K. However, the number of Brønsted acid sites is reduced sharply with further increase in hydrothermal treatment temperature. The Lewis acid sites are affected only slightly by the temperature of hydrothermal treatment. HTM-8 exhibits a very significant improvement in EB selectivity together with a slight decrease in benzene conversion compared with parent MCM-22. The increase in EB selectivity may be due to suppression of side reactions such as benzene multi-alkylation and ethylbenzene cracking, with decline in Brønsted acid sites. It can also be concluded that alkylation of benzene with DEC occurs mainly on Brønsted acid sites, and the effect of Lewis acid sites on the alkylation process is negligible. The activity of benzene alkylation with DEC is reduced severely over HTM-9 and HTM-10, indicating that a particular acidity strength of catalyst is required to maintain high benzene conversion and EB selectivity.

Acknowledgments

We deeply appreciate the financial support from the high technology research and development program of Jiangsu province (BG2006015) and the foundational research project of department of education of Jiangsu province (06KJA5013).

References

[1] M.E. Leonowicz, J.A. Lawton, S.L. Lawton, M.K. Rubin, Science 264 (1994) 1910–1913.
[2] R. Ravishankar, D. Bhattacharya, N.E. Jacob, S. Sivasanker, Micropor. Mater. 4 (1995) 83–93.
[3] M.A. Asensi, A. Corma, A. Martinez, J. Catal. 158 (1996) 561–569.
[4] P. Wu, T. Komatsu, T. Yashima, Micropor. Mesopor. Mater. 22 (1998) 343–356.
[5] N. Kumar, L.E. Linddfors, Appl. Catal. A: Gen. 147 (1996) 175–187.
[6] P. Chu, M.E. Landis, Q.N. Le, U.S. Patent 5,334,795 (1994).
[7] A. Corma, V. Martinez-Soria, E. Schnoeveld, J. Catal. 192 (2000) 163–173.
[8] V.R. Vijayaraghavan, K.J.A. Raj, J. Mol. Catal. A: Chem. 207 (2004) 41–50.
[9] K.J.A. Raj, E.J.P. Malar, V.R. Vijayaraghavan, J. Mol. Catal. A: Chem. 243 (2006) 99–105.
[10] Y.M. Wei, G. Wu, Y. Fan, L.C. Liu, Energy Econ. 30 (2008) 290–302.
[11] T.F. Degnan Jr., C.M. Smith, C.R. Venkat, Appl. Catal. A: Gen. 221 (2001) 283–294.
[12] Z. Zhang, X.B. Ma, P.B. Zhang, Y.M. Li, S.P. Wang, J. Mol. Catal. A: Chem. 266 (2007) 202–206.

[13] Z. Zhang, X.B. Ma, J. Zhang, F. He, S.P. Wang, J. Mol. Catal. A: Chem. 227 (2005) 141–146.
[14] R.L.V. Mao, T.M. Nguyen, J. Yao, Appl. Catal. A: Gen. 61 (1990) 161–167.
[15] E.V. Sobrinho, D. Cardoso, E. Fababella, J.G. Silva, Appl. Catal. A: Gen. 127 (1995) 157–164.
[16] R.Q. Lv, Q.Y. Wang, S.H. Xiang, Chin. J. Catal. 23 (2002) 421–424.
[17] P. Zhang, X.S. Wang, X.W. Guo, L. Zhao, Y. Hu, Catal. Lett. 92 (2004) 63–68.
[18] C.H. Ding, X.S. Wang, X.W. Guo, S.G. Zhang, Catal. Commun. 9 (2007) 487–493.
[19] A. Corma, V. Fornes, J.M. Triguero, S.B. Pergher, J. Catal. 186 (1999) 57–63.
[20] Y.C. Shang, P.P. Yang, M.J. Jia, W.X. Zhang, T.H. Wu, Catal. Commun. 9 (2008) 907–912.
[21] S.J. Wang, J. Liang, G.W. Guo, L.Q. Zhao, R.H. Wang, Chin. J. Catal. 13 (1992) 38–43.
[22] S. Unverrichet, M. Hunger, S. Ernst, H.G. Karge, J. Weitkamp, Stud. Surf. Sci. Catal. 84A (1994) 37–44.
[23] G. Dahlhoff, U. Barsnick, W.F. Holderich, Appl. Catal. A: Gen. 210 (2001) 83–95.
[24] G.S. Kumar, S. Saravanamurugan, M. Hartmann, M. Palanichamy, V. Murugesan, J. Mol. Catal. A: Chem. 272 (2007) 38–44.
[25] P. Meriaudeau, V.A. Tuan, V.T. Nghiem, F. Lefevbre, V.T. Ha, J. Catal. 185 (1999) 378–385.
[26] I. Guray, J. Warzywoda, N. Bac, A. Sacco Jr., Micropor. Mesopor. Mater. 31 (1999) 241–251.
[27] A. Corma, U. Diaz, V. Fornes, J.M. Guil, J.M. Triguero, E.J. Ceyghtony, J. Catal. 191 (2000) 218–224.
[28] N. Kumar, R. Byggningsbacka, M. Korpi, L. Linfors, T. Salmi, Appl. Catal. A: Gen. 227 (2002) 97–103.
[29] S. Kumar, A.K. Sinha, S.G. Hegde, S. Sivasanker, J. Mol. Catal. A: Chem. 154 (2000) 115–120.
[30] P.A. Jacobs, H.K. Beyer, J. Phys. Chem. 83 (1979) 1174–1177.
[31] S.M. Campbell, D.M. Bibby, J.M. Coddington, R.F. Howe, R.H. Meinhold, J. Catal. 161 (1996) 338–349.
[32] S.C. Shen, S. Kawi, Langmuir 18 (2002) 4720–4728.
[33] A. Martin, U. Wolf, S. Nowak, B. Lucke, Zeolites 11 (1991) 85–87.
[34] R.D. Shannon, K.H. Gardner, R.H. Stadey, G. Bergeret, P. Gallezot, A. Auroux, J. Phys. Chem. 89 (1985) 4778–4788.
[35] W.P. Zhang, X.W. Han, X.M. Liu, X.H. Bao, J. Mol. Catal. A: Chem. 194 (2003) 107–113.
[36] Y.C. Du, H. Wang, S. Chen, J. Mol. Catal. A: Chem. 179 (2002) 253–261.
[37] V. Mavrodinova, M. Popova, R.M. Mihalyi, G.P. Borbely, C. Minchev, Appl. Catal. A: Gen. 248 (2003) 197–209.
[38] X.X. Guan, N. Li, G.J. Wu, J.X. Chen, F.X. Zhang, N.J. Guan, J. Mol. Catal. A: Chem. 248 (2006) 220–225.
[39] K.U. Nandhini, B. Arabindoo, M. Palanichamy, V. Murugesan, Catal. Commun. 7 (2006) 351–356.
[40] L.Y. Xu, Q.X. Wang, W.C. Liu, S.J. Xie, X.D. Sun, J. Bai, S.R. Zhang, C.D. Dong, Chin. J. Catal. 24 (2003) 73–78.
[41] Y.C. Fu, H.Y. Zhu, J.Y. Shen, Thermochim. Acta 434 (2005) 88–92.
[42] W.B. Kim, Y.G. Kim, J.S. Lee, Appl. Catal. A: Gen. 194–195 (2000) 403–414.